Q. J. R. Meteorol. Soc. (1997), **123**, pp. 727–741

Identification of cyclone-track regimes in the North Atlantic

By R. BLENDER, K. FRAEDRICH* and F. LUNKEIT
Meteorologisches Institut, Universität Hamburg, Germany

(Received 2 January 1996; revised 5 June 1996)

SUMMARY

A Langrangian-type climatology of North Atlantic cyclones is established based on the high-resolution European Centre for Medium-Range Weather Forecasts data-set of the 1000 hPa height-field. First, an algorithm is introduced to identify mid-latitude cyclones and cyclone paths with as few constraints as possible. Cluster analysis of relative cyclone displacements yields three types of cyclone tracks characterizing stationary-, north-eastward- and zonally-travelling storms. The internal Lagrangian statistics of these cyclone-track types reveal representative life-cycles for central pressure and geopotential-height gradients and a power-law scaling behaviour of cyclone displacements. Finally, a basic climatology of North Atlantic cyclone-track regimes is deduced in terms of a time-series and circulation statistics.

KEYWORDS: Cluster analysis Cyclone classification Lagrangian climatology

1. INTRODUCTION

Meteorological observations are analysed to provide physical information concerning, for example, the energy and momentum budgets of the atmospheric dynamics and their properties in space-time or wavenumber-frequency domains. Another type of data analysis is the phenomenological circulation statistics of structurally-stable processes, which are related to real weather systems. The Grosswetterlagen in the European–North Atlantic region and the British Isles weather (Lamb 1972; Hess and Brezowski 1977) have been analysed ever since weather maps became available, and extra-tropical cyclones and their tracks have been extracted subjectively (for example, van Bebber 1891; Hay 1949; Klein 1957) or automatically (Lambert 1988; Alpert *et al.* 1990; Hodges 1994; and others). Both physical and phenomenological analyses describe the same processes and contribute different aspects to them. Traditional and nonlinear time-series analyses complement the phenomenological approach in the sense that, for example, scaling properties can be deduced, as Richardson (1926) did in his diffusion experiments using parsnips on the sea surface.

In this paper the phenomenology of mid-latitude cyclone tracks is revisited. Mid-latitude cyclones form an integral part of the atmospheric climate system. They undergo a life-cycle during which they follow more or less well-defined paths, defined as cyclone or storm tracks. They are associated with rain-bearing frontal weather systems affecting regional climates and in particular the water-cycle and the weather extremes.

There are two main areas in the northern hemisphere whose climate is dominated by the influence of these synoptic-scale systems: the North Atlantic and European sector and the North Pacific. The climate of the European area is characterized by the cross-Atlantic cyclone track. In particular, the sensitivity of the tail-end of this cyclone track, which is associated with the final stages of the cyclones' life-cycles, dominates the weather and climate variability over the European continent. About 70–80% of the winter precipitation in continental Europe originates from about 15 frontal cyclones (Fraedrich *et al.* 1986). Storm tracks interact with the Atlantic Ocean and can be affected by distant atmospheric events, like the El Nino in the tropical Pacific. Thus, climate variability and the variability of the intensity and location of the dominating storm tracks are closely linked.

The purpose of this paper is to present a Lagrangian-type climatology of the North Atlantic cyclones based on a high-resolution European Centre for Medium-Range Weather

* Corresponding author: Meteorologisches Institut der Universität Hamburg, Bundesstraße 55, D-20146 Hamburg, Germany.

Forecasts (ECMWF) data-set (of the 1000 hPa height field). Compared to the variability analyses by standard Eulerian storm-track diagnostics which is based on filtered geopotential-height variance, our approach explicitly considers the weather systems which cause the variability.

First, an algorithm is introduced to identify mid-latitude cyclones and cyclone paths with as few constraints as possible (section 2). Relative cyclone displacements obtained by this algorithm are analysed to yield cyclone-track clusters (section 3). The internal Lagrangian statistics within representative clusters are evaluated (section 3). Finally, the North Atlantic cyclone-track regimes and their climatology are deduced to complete the picture (section 4). The outlook (section 5) suggests model validation and inter-comparison as possible future applications of the methods presented here.

2. Data analysis: cyclones and cyclone tracks

In order to ensure high reliability of the results obtained by a cyclone-tracking algorithm, data with high temporal and spatial resolution are required. Therefore, we chose the ECMWF analyses, which are available at six-hour intervals and T106 horizontal resolution (about $1.1° \times 1.1°$), between 1990 and 1994. This data-set is relatively short but it shows no distinct deviation from a long-term climatological mean with respect to the traditional Eulerian variance measure given by the band-pass filtered 500 hPa geopotential-height variance. The area selected for storm-track analysis spans the North Atlantic from eastern North America to western Europe between 80°W–30°E longitude and 30°N–80°N latitude; the winter seasons are extended from November through March, the first winter being restricted to January–March 1990.

The cyclone-identification algorithm follows a standard approach (for example, Lambert 1988; Bell and Bosart 1989; Alpert *et al.* 1990; Koenig *et al.* 1993; Ueno 1993) and is designed as a minimal procedure consisting of only two steps: (1) A cyclone is defined as a surface-pressure low and therefore identified as a local minimum of the 1000 hPa geopotential-height reference field, z1000. This local minimum should occur within an area covering 3×3 grid points (independent of latitude). (2) The only additional condition on this minimum is a measure of intensity: a positive mean gradient of the z1000 height is required in a 1000×1000 km^2 area about the minimum corresponding to the Rossby-deformation scale. These rather weak conditions enable us to detect cyclones already at the initial stage of the life-cycle. The requirement of a closed isobar in a synoptic region which, for example, was used by Koenig *et al.* (1993) would preclude such weak phenomena.

Due to the high horizontal resolution of the data it is not necessary to introduce a spatial interpolation scheme to define optimal sub-grid positions of cyclones, as was necessary for Alpert *et al.* (1990) and Murray and Simmonds (1991). Maxima in the vorticity are not considered because the structure of this field is too detailed and noisy in high-resolution data. This leads to severe problems in a tracking procedure which are not met in the geopotential field. However, the vorticity field appears to be useful for lower resolution as described in the T21-analysis of Koenig *et al.* (1993) or in the T42-analysis of Hodges (1994). One disadvantage of using the surface geopotential height needs to be mentioned. Disconnected isobars may occur due to a large pressure gradient superimposed by the large-scale flow (as illustrated in Fig. 1 of Sinclair 1994), although a vorticity maximum is present. This is relevant in the initial small-amplitude phase of the cyclonic activity. However, this effect is assumed to be weak at the surface and, therefore, it is not considered in the cyclone-tracking procedure.

The trajectories are determined by a simple nearest-neighbour search in the preceding z1000 field without assuming a preferred propagation direction and speed. A maximum

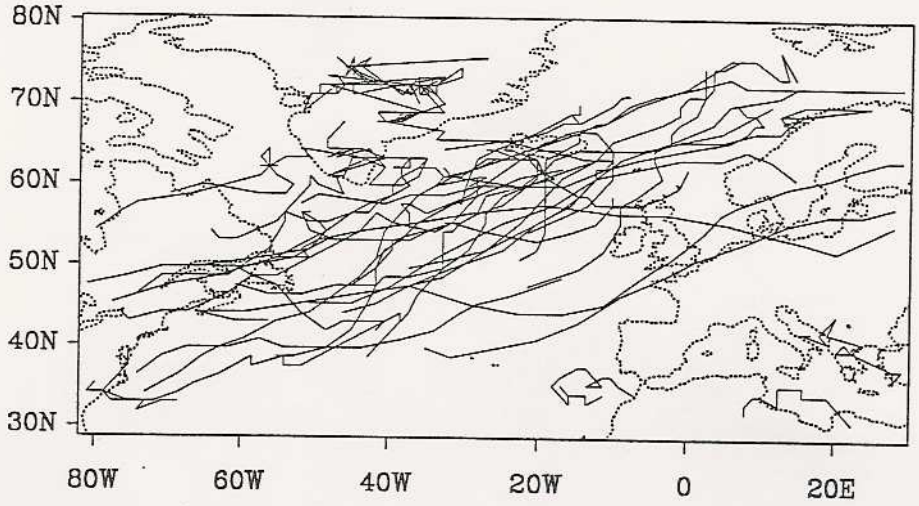

Figure 1. Paths of cyclones with a minimum lifetime of $T = 3$ days (November 1990 to March 1991).

displacement velocity of about 80 km h^{-1} restricts the range of motion, but this condition is rarely needed. The method has been compared with a subjective analysis and reveals identical results.

The trajectory X_j of an individual cyclone j is a sequence of cyclone positions $[x_j(t), y_j(t)]$, for successive time-steps $t = 0, \ldots, T$, observed at 6-hourly time-intervals commencing at the initial detection

$$X_j = [x_j(t=0), y_j(t=0), \ldots, x_j(t=T), y_j(t=T)]. \tag{1}$$

Application of the identification algorithm to the five winters yields 449 cyclones with a lifetime of $T = 3$ days and longer. The largest number is located around Greenland and the Mediterranean Sea. Figure 1 shows the paths of all cyclones in the second winter, November 1990 to March 1991. It should be noted that, due to the geographical area being limited to the North Atlantic, cyclones penetrating the boundaries (near the end or at the beginning of their life-cycle) may not exceed the $T = 3$ days threshold. Thus, under-estimation of cyclone frequencies near the boundaries (over eastern North American and western Europe) cannot be excluded. Since we are interested in the cyclones whose life-cycles affect the climatology of the North Atlantic region, these boundary effects are not considered.

3. Cluster analysis and cyclone track clusters

The trajectories X_j of the individual cyclones are subjected to a cluster-analysis algorithm to yield storm-track regimes which, after suitable sample averaging, characterize cyclones of similar travel speed and direction. Cyclone locations relative to their initial position, $[x_j(0), y_j(0)]$, contain this information, whereas clusters averaged over absolute positions provide nearest neighbours at preferred locations. Therefore, the relative displacements,

$$d_j(t) = [\mathrm{d}x_j(t), \mathrm{d}y_j(t)] = [x_j(t) - x_j(0), y_j(t) - y_j(0)] \tag{2}$$

given in geographical distances, will be further analysed to extract regime-like behaviour. This requires that all individual cyclones are represented by the same (minimum) lifetime T, $D_j = [d_j(t=0), \ldots, d_j(t=T)]$. The remaining parts of the trajectories are not considered in the cluster analysis. The threshold $T = 3$ days appears to be reasonable. A

longer limit of the minimum lifetime reduces the number of cyclones thereby reducing the statistical significance of the results. On the other hand the separation of different cyclone tracks becomes less significant for shorter lifetimes. A more detailed discussion follows later in this section.

Formally, a time trajectory of an individual cyclone can be interpreted as a single point in a phase space of time-delay coordinates spanned by the consecutive cyclone displacements, $[\mathrm{d}x(t=6h), \mathrm{d}y(t=6h), \ldots, \mathrm{d}x(t=T), \mathrm{d}y(t=T)]$. Accordingly, cyclone-track regimes or clusters can be interpreted as ensembles of suitably weighted neighbouring points in this phase space. The subsequent cluster analysis identifies such regime-like behaviour in terms of cyclone displacements.

(*a*) *Cluster analysis*

The relative $\mathrm{d}x_j$ and $\mathrm{d}y_j$ coordinates are scaled by their respective standard deviation. As the variance in zonal direction is larger, this normalization gives more weight to the meridional displacements. The cluster analysis is performed by the K-means algorithm (Hartigan and Wong 1979) using the numerical IMSL-library. The K-means algorithm is usually applied as an optimizing procedure after agglomerative or hierarchical cluster-algorithms have been applied. We choose this method because it provides a mathematically-transparent and simply-applicable algorithm. For a given number, K, of clusters, this method minimizes the sum, S, of the squared distances within the clusters

$$S = \sum_{i=1}^{N} \sum_{j=1}^{M} (z_{i,j} - w_{k(i),j})^2. \tag{3}$$

Divided by N, this measures the average squared Euclidean distance of all relative cyclone trajectories to their corresponding cluster centres in the time-delay coordinate phase space. The index i counts the N cyclones, z denotes both scaled coordinates of the relative displacements $[\mathrm{d}x, \mathrm{d}y]$, the index j counts these variables with a total number $M = 24$ (for 12 time-steps and two coordinate directions). The K-means algorithm modifies the grouping $k(i)$ (where $k = 1, \ldots, K$) dynamically, that is by swapping points between clusters, in order to find the minimum of S. For the k-th cluster, $w_{k,j}$ is the mean of the variables $z_{i,j}$

$$w_{k,j} = \frac{1}{N_k} \sum_{i \epsilon C_k} z_{i,j} \tag{4}$$

for the cyclones i in this cluster C_k. N_k denotes the occupation number, which is the total number of cyclones within C_k.

The result of the K-means algorithm may depend on the initial seed because local minima may occur. Therefore, the calculations are repeated 20 times using different seeds out of the available set of relative trajectories and the global minimum was taken as the result. However, local minima rarely occur (roughly 10%) and almost all of the seeds yield the identical result which is then assumed to represent the global minimum.

Sensitivity experiments are performed with the cluster algorithm for different numbers K of clusters and minimum lifetimes T of cyclones. Based on these results, the optimal values for K and T are determined using meteorological considerations described below in some detail. The algorithm is applied using a set of threshold values $T = 2, 3, 4$ days (minimum cyclone age affecting the trajectory length) and a number of clusters ranging from $K = 2$ to 6. Selected results are shown in Fig. 2 presenting centroids in terms of the mean relative displacements for each cluster (in units of 1000 km); meridional and zonal error-bars denote standard deviations and are marked daily.

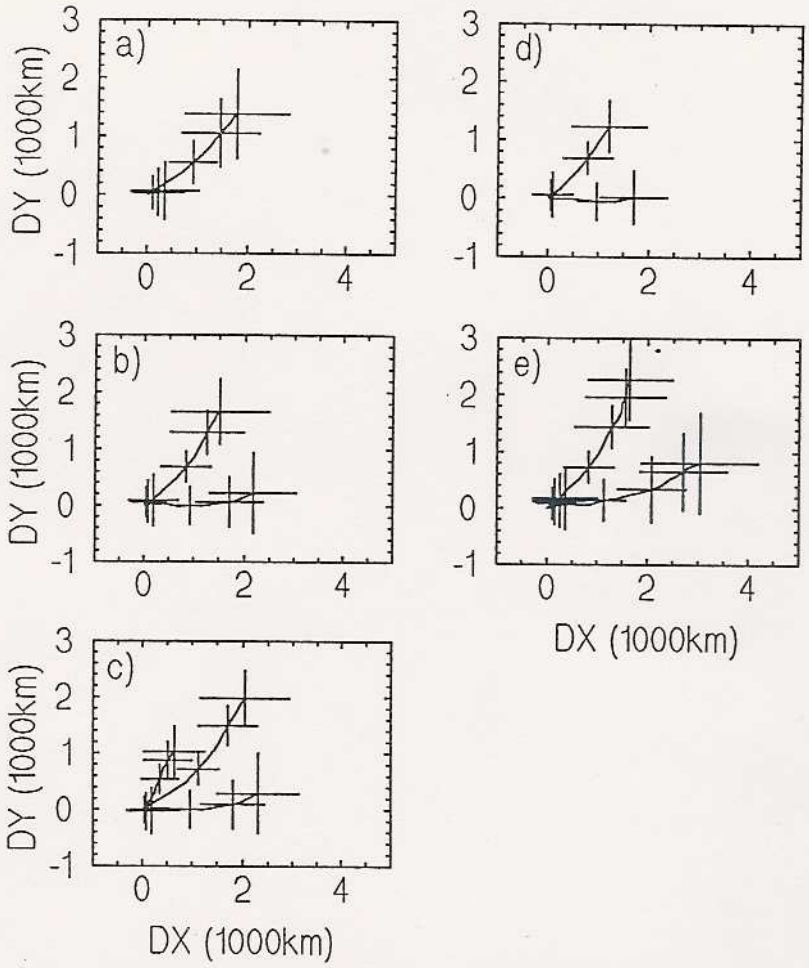

Figure 2. Centroids of the cyclone trajectories with a minimum age of $T = 3$ days for various cluster numbers: (a) $K = 2$, (b) $K = 3$, (c) $K = 4$; the age-dependence is shown for cluster number $K = 3$ for (d) $T = 2$ days and (e) $T = 4$ days. Error-bars are drawn daily and denote the standard deviation in zonal and meridional directions.

• For cyclones exceeding the $T = 3$ day lifetime threshold, $K = 2$ clusters reveal a nearly stationary group of cyclones while the other group is composed of north-eastward travelling storms (Fig. 2(a)). Obviously, the cluster analysis extracts quasi-stationary cyclones which could have been eliminated before by using a subjective threshold value for the maximum displacement. For $K = 3$ (Fig. 2(b)), the cluster of moving cyclones splits into a north-eastward and a zonally propagating branch. The missing overlap of error-bars indicates that a distinct separation of the groups has been attained. For $K = 4$ (Fig. 2(c)), an additional cluster of slowly-northward-moving cyclones is created; this group is a mixture of stationary and north-easterly cyclones emerging from $K = 3$. The cluster of zonally propagating storms, however, is not altered by increasing K from 3 to 4.

• Now, the dependence on the cyclone age ($T = 2$ and 4 days) is evaluated, keeping the number of $K = 3$ clusters fixed (Figs. 2(d) and (e)). Here, for $T = 2$, we recognize a distinct separation of the cyclones clustering according to their direction of travel (Fig. 2(d)); these patterns hardly change when analysing $T = 3$ and 4 days (Figs. 2(b) and (e)). Note that the mean propagation-velocity in the centroids decreases with the lifetime of the cyclones; this can be detected by the naked eye from the decreasing distances between error-bars set at fixed time-intervals.

Corroborating these sensitivity experiments, the minimum age of $T = 3$ days and a number of $K = 3$ clusters provide a distinct separation of cyclone tracks according to their

propagation direction. The three clusters will be denoted as 'stationary', 'north-eastward' and 'zonal' cyclone-track regimes, which are further analysed in the following.

(*b*) *Cyclone-track clusters*

The actual geographical positions of the cyclones in the three clusters are presented in Fig. 3 showing the stationary cyclones (Fig. 3(a)), the north-eastward-travelling (Fig 3(b)) and the zonal cyclones (Fig. 3(c)). The complete trajectories are plotted; their length is not confined to the initial $T = 3$ day time-span.

The stationary cyclones are predominantly located around Greenland and in the Mediterranean Sea. Note that in the southern North Atlantic a few cyclones occur which are classified as stationary, because they behave like stationary cyclones during the first $T = 3$ days. Later in their life-cycle, however, they propagate like the typical north-eastward-travelling cyclones. The north-eastward cyclones (Fig. 3(b)) are located in the region of the North Atlantic storm track. The zonal cyclones originate in the same region as the north-eastward ones, but propagate zonally towards England and Europe. It is noteworthy that the cluster analysis, successfully applied to cyclone displacements leads also to geographically-meaningful cyclone-track patterns.

The occupation numbers are 254 (stationary), 123 (north-eastward) and 72 (zonal), respectively (Fig. 4). After 3 days the occupation numbers decay approximately with the same rate (0.6 per day) for all clusters. Independent of the cluster, the mean lifetime of the cyclones is about 4.5 days.

4. Internal variability: life-cycles and power-law scaling

The time evolution of physical-state variables and of geometrical-propagation parameters, like the relative displacements, characterize the internal variability of the travelling cyclones comprised in a single cluster. This leads to a representative life-cycle and provides a power-law scaling behaviour of the cyclone paths, treated as diffusive elements in a large-scale flow.

The life-cycle of baroclinic disturbances is more or less well-defined by the time evolution of the minimum z1000 height and a representative z1000 gradient. These cluster-averaged cyclone life-cycles are presented in Fig. 5 for the first four days of the time evolution: cyclones of the north-eastward cluster show a pronounced life-cycle of both the z1000 geopotential height (Fig. 5(right)) and its gradient (Fig. 5(left)). The zonally travelling cyclones have a clear but weak life-cycle and the stationary cyclones show none. As the number of cyclones decreases after the $T = 3$ days threshold these results appear to be less robust.

The transport properties of turbulent geophysical flows are typically characterized by anomalous diffusion (Fraedrich and Leslie 1989; Fraedrich *et al.* 1990, adopting the Richardson diffusion experiment for tropical and mid-latitude cyclones; see Tsinober 1994, for a review). Treating travelling cyclones as large-scale diffusive elements, they obey a fractional power-law scaling of the time behaviour of the mean squared displacements (normalized by appropriate standard deviations):

$$\langle \mathrm{d}x^2(t) + \mathrm{d}y^2(t) \rangle \sim t^q. \tag{5}$$

The mean square displacement is calculated for the whole set of cyclones as well as for the different clusters. Figure 6 shows power-law scaling of the total, zonal and meridional displacements in log–log format: $\langle \mathrm{d}x^2 + \mathrm{d}y^2 \rangle$, $\langle x^2 \rangle$, $\langle y^2 \rangle$ for the upper, middle and lower curves. The average of all cyclones yields $q = 1.52$, the north-eastward cyclones

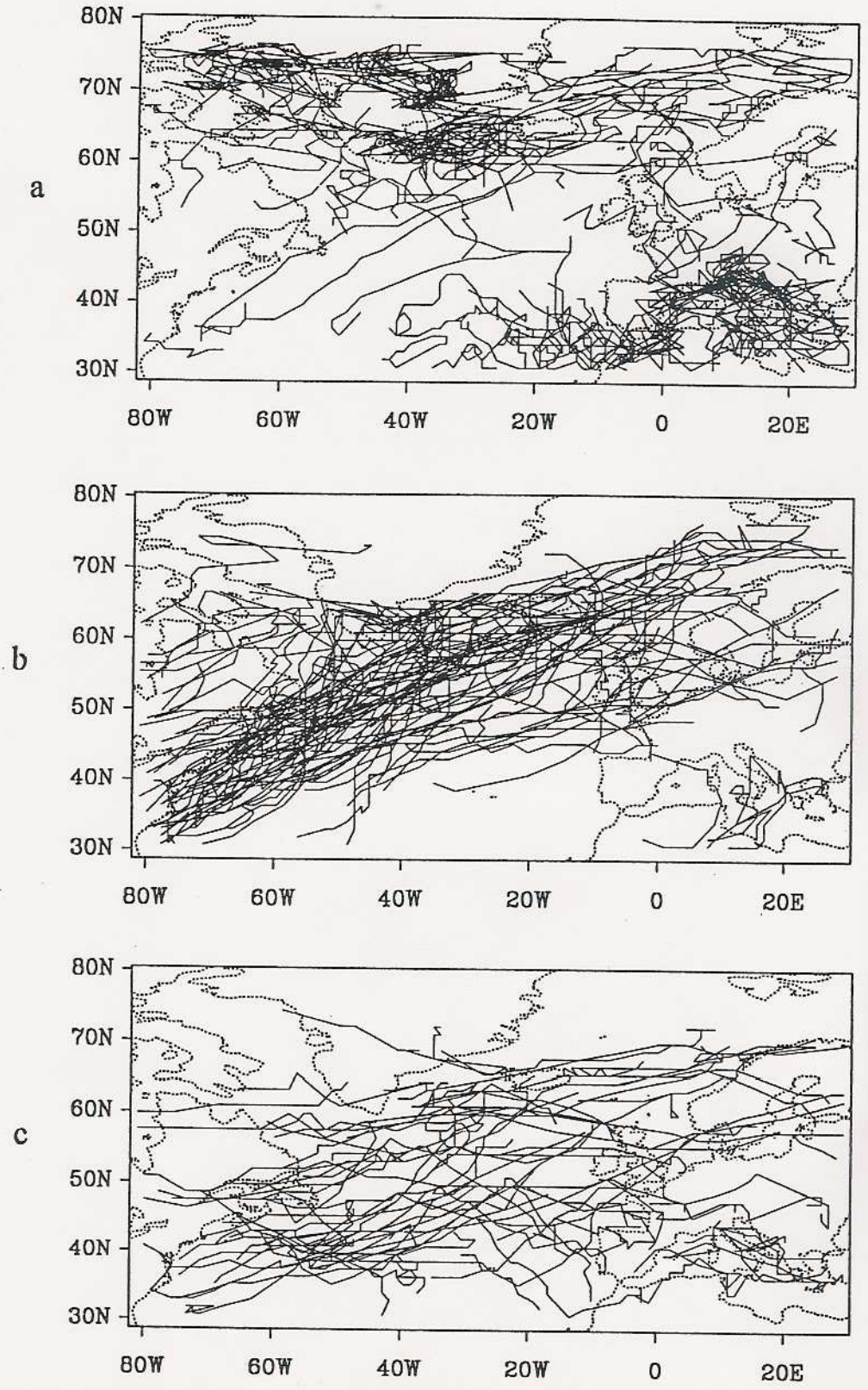

Figure 3. Cyclone tracks represented by (a) stationary, (b) north-eastward and (c) zonal clusters.

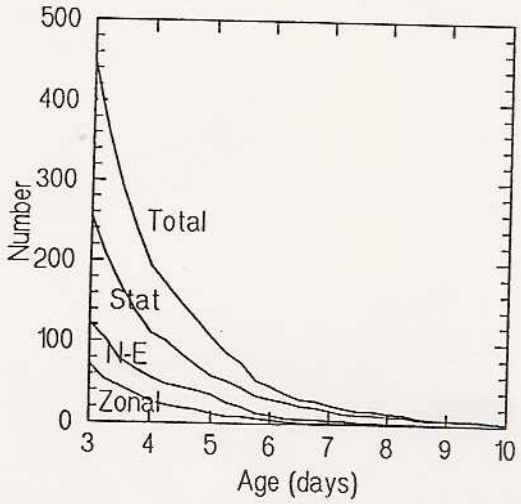

Figure 4. Time-dependent occupation numbers of the three clusters (denoted by the corresponding cyclone type) as well as the total number for cyclones with a minimum lifetime of three days.

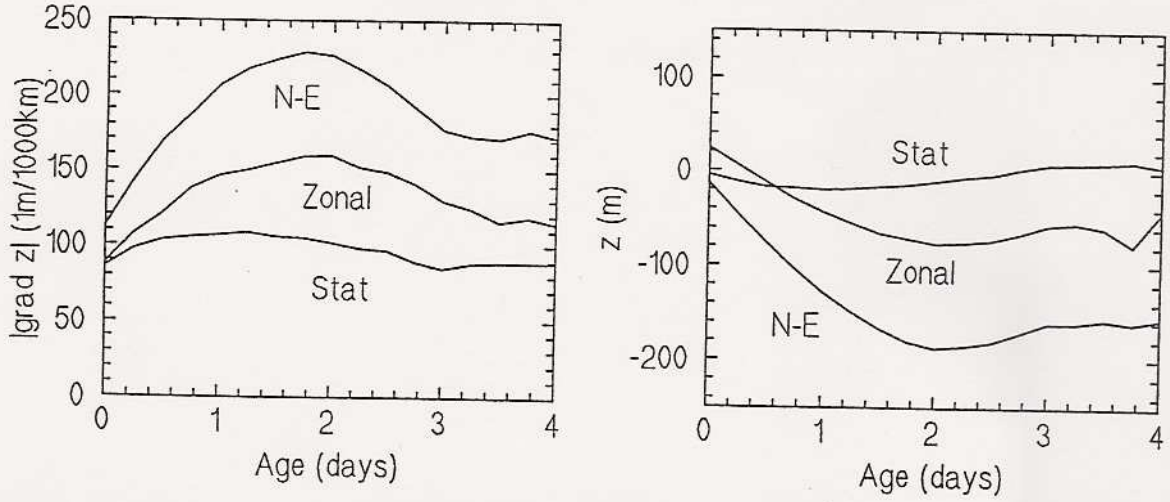

Figure 5. Average life cycle of cyclones in the north-eastward and zonal cyclone-track clusters: 1000 hPa height gradient and height.

$q = 1.67$, and the zonal cyclones $q = 1.59$. The stationary cyclones follow purely diffusive behaviour like a random walk with $q = 1$. The motion of the north-eastward and zonal cyclones is neither purely linear, $q = 2$, nor diffusive, $q = 1$.

In general one observes $1 < q < 2$ for geophysical flows. Such a behaviour is related to a trajectory of a non-integer fractal dimension $d = 2/q$. The curves show statistical self-similarity when considered on different length scales. Our results coincide with findings of other authors: Sanderson and Booth (1991) measured $d \approx 1.3$ ($q \approx 1.5$) for drifter trajectories. Viecelli (1994) obtained $q = 1.67$ in a simple point-vortex model for the mid-latitude circulation. Thus, our results provide additional support for the universality of the exponent $q \approx 1.5$.

A useful application of the analysis of the power-law exponent q pertains to the quality check of cyclone-tracking algorithms. Erroneously tracked cyclones are similar to random walks. Therefore, a result $q \approx 1$ for cyclones propagating over large distances may hint at a wrong tracking method.

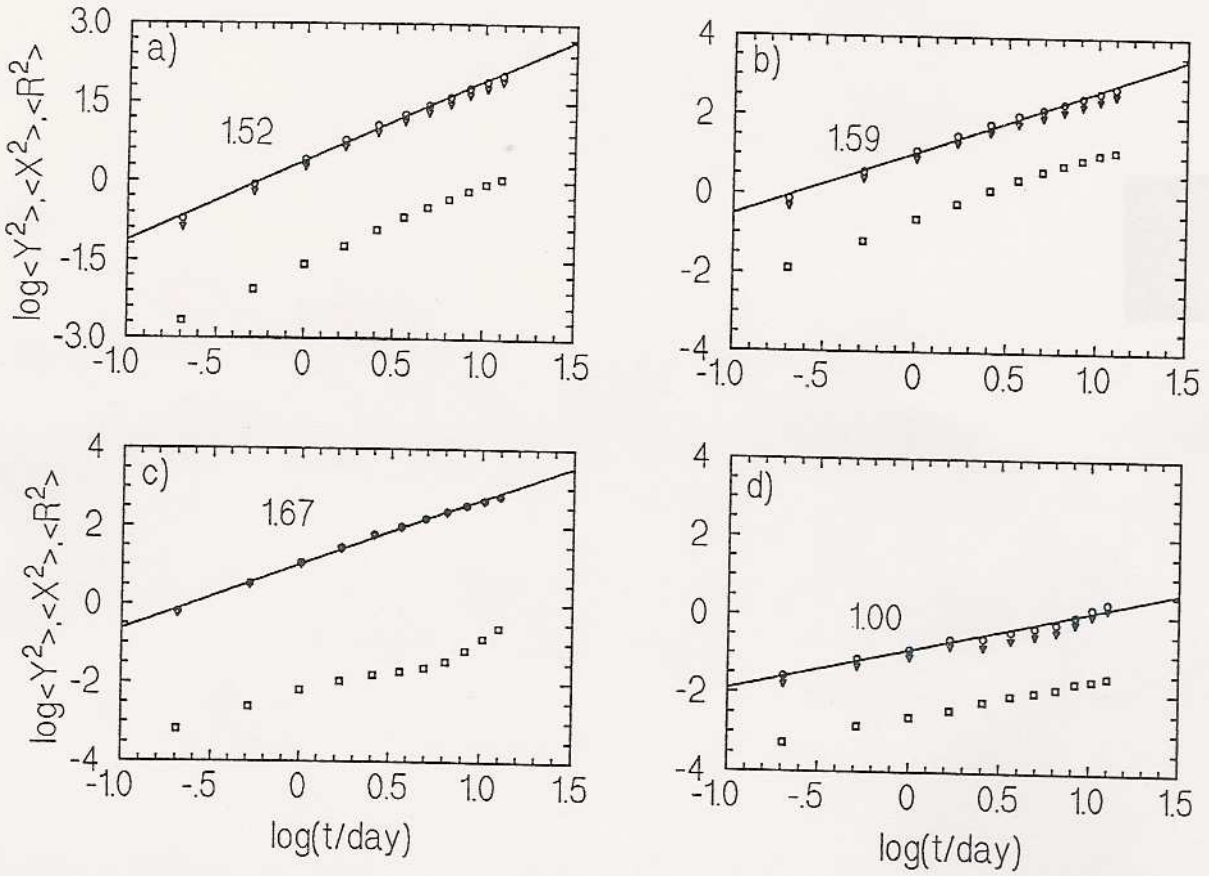

Figure 6. Power-law scaling of the total, zonal and meridional displacements in log–log format: $\langle dx^2 + dy^2 \rangle$, $\langle x^2 \rangle$, $\langle y^2 \rangle$ for the upper, middle and lower curves. The scaling is shown for (a) the total number of cyclones, and for (b) the north-eastward, (c) the zonal and (d) the stationary clusters.

5. Climatology of cyclone-track regimes: Time statistics and mean flow

A climatology of the North Atlantic can be established based on the results of the cluster analysis. This climatology is associated with the north-eastward and the zonal clusters of relative trajectories which were identified as a consistent separation of travelling cyclones (section 3). Stationary cyclones are excluded in the following. Principal cyclone tracks associated with these two clusters are determined by meridional-position averaging (Fig. 7). A time-series of three mutually-exclusive states is constructed to characterize regimes of cyclonic activity over the North Atlantic. On a day to day basis the dominating cyclone-track cluster (section 3) is identified by the largest number of cyclones present. Each day is classified as 'north-eastward' or 'zonal' cyclone-track regime (or state). Regime persistence prevails if two clusters are found to have equal numbers of cyclones on the same day. If no travelling cyclones are present, an 'inactive' cyclone regime is assigned to that day. Figure 8 shows the regime time-series obtained for the winter 1990/91. Due to the higher number of north-eastward-travelling cyclones, this state occurs most frequently. Both cyclone-track regimes have a persistence of a few days.

The time variability of the North Atlantic cyclone-track regimes is characterized by the distributions of their residence times, which are the time-intervals of uninterrupted dominance of one cluster (Fig. 9). Note that these residence times are not directly related to the lifetimes of the individual cyclones. The north-eastward state (Fig. 9(a)) shows a broad distribution with a mean residence time of about 5 days; short periods of one and two days are not observed, which is only partly due to the large number of cyclones in this regime. The zonal state (Fig. 9(b)) shows an equally broad distribution but with a smaller

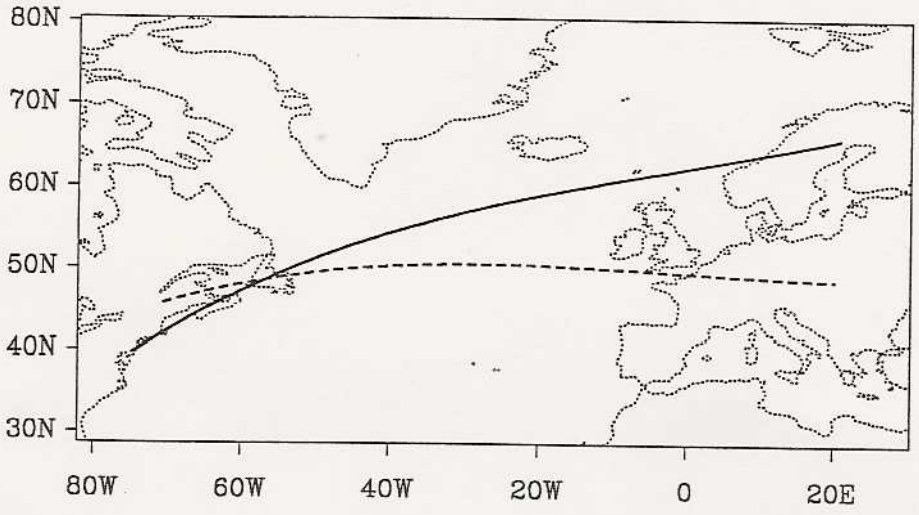

Figure 7. Principal traces of the cyclone positions in the north-eastward (solid) and the zonal (dashed) clusters.

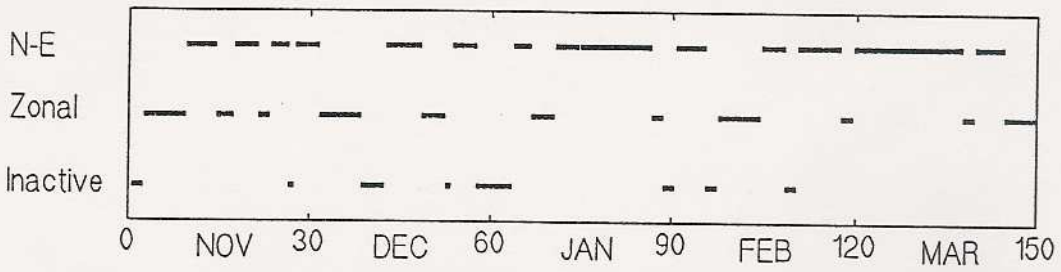

Figure 8. Sample time-series of North Atlantic cyclone-track regimes: north-eastward, zonal and inactive (from top to bottom) from November 1990 through March 1991.

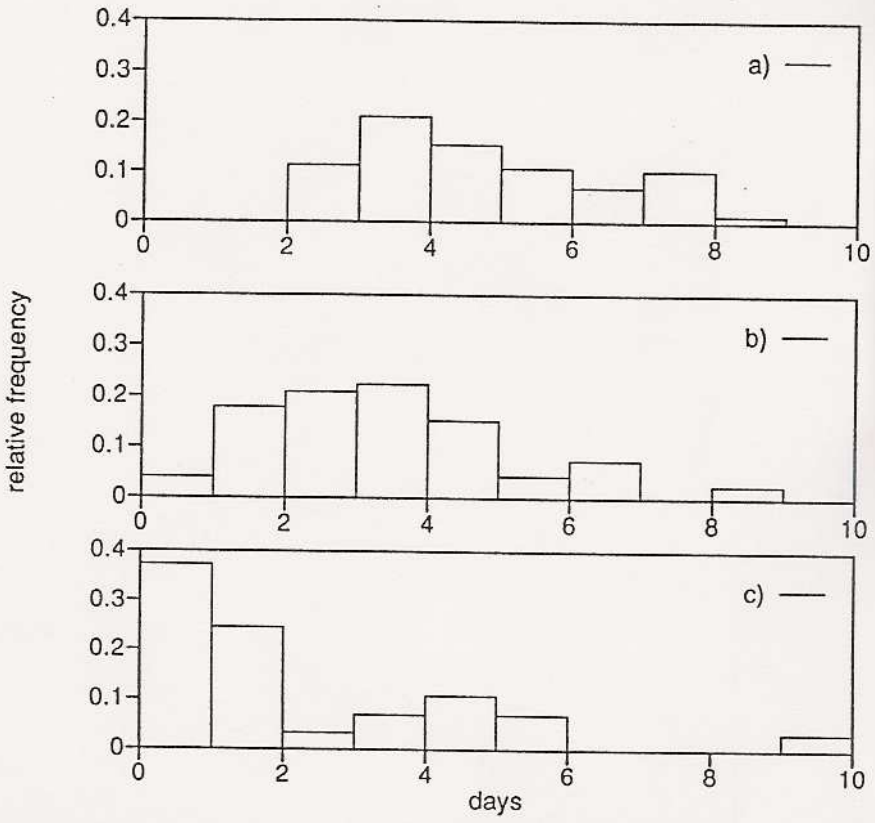

Figure 9. Residence time distribution of cyclone-track regimes over the North Atlantic. Relative frequencies of the occurrence of regimes occupying a successive number of days (residence time): (a) north-eastward, (b) zonal and (c) inactive.

mean of four days. It is remarkable that this state is rather persistent although the total number of zonal cyclones is smaller than of north-eastward cyclones. Finally, the inactive regime (Fig. 9(c)) shows a bi-modal distribution with peaks at one and five days. The first peak can be related to the transition periods between the zonal and north-eastward regime, while the longer periods are attributed to anticyclonic situations over the North Atlantic.

A circulation climatology can also be associated with these cyclone-track regimes. Composite fields of the z1000 geopotential height and the 850 hPa temperature are constructed from regime- or cyclone-state time-series (Fig. 8). Averaging the daily fields for the three regimes yields three z1000 composites presented in Fig. 10. Figure 10(a) shows the five-winter average, while Figs. 10(b), (c) and (d) present the mean anomaly during the north-eastward, the zonal, and the inactive regimes, respectively. In general, depressions occur in the regions where the cyclones are located. The north-eastward anomaly is observed in the northern part between 50 N and 60 N, the zonal anomaly occurs in the more southern area of the North Atlantic, and the inactive anomaly shows an anticyclonic circulation centred along 50 N.

The temperature anomalies are presented in Fig. 11. The north-eastward-cluster regime shows an enhanced land–ocean temperature difference associated with an intensification of the meridional temperature gradient between 40 N and 50 N. In the zonal regime the land–ocean temperature contrast is reduced and the inactive days are characterized by a warm anomaly to the west of the anticyclone (Fig. 10(c)) and relatively cold continents.

6. Conclusion and discussion

Cyclone tracks in the North Atlantic/European region have been determined for extended winter periods between 1990 and 1994 using high-resolution ECMWF analyses. The algorithm applied is designed to be as simple and transparent as possible to obtain reproducible results.

A cluster analysis of the relative trajectories of the cyclones leads to a classification of three distinctly different groups of stationary, zonally and north-eastward-travelling storms. These three clusters differ in the physical and geometrical properties of their cyclones as shown by the geographical positions, the life-cycles and the mean-squared displacements.

The kinematic behaviour of travelling cyclones is consistent with observations of two-dimensional geophysical flows; the result agrees remarkably well with a simple barotropic point-vortex model. The stationary cyclones reveal purely diffusive behaviour associated with linear mean-squared displacements that cannot be distinguished from an erroneous tracking procedure. Furthermore, an analysis of the mean-squared displacements of cyclones may provide a simple test for the quality of tracking algorithms. In this sense, erroneously tracked cyclones can, in principle, be identified and thus eliminated using this procedure. That is, stationary cyclones classified by their mean-squared displacement could have been excluded (as purely diffusive systems) prior to the cluster analysis.

A novel approach for a climatology is established. It is linked to the Lagrangian properties of cyclones and based on the dominant occupation time of the three clusters. In this manner cyclone-track regimes over the North Atlantic are related to distinct circulation patterns. For Europe we observe that the zonal regime is not correlated with European Grosswetterlagen (updated from Hess and Brezowski 1977), whereas there is a correlation between the regime of north-eastward-travelling cyclones over the North Atlantic and the anti-cyclonic synoptic situations over Europe. It will be worth applying this approach to the longer re-analysed ECMWF data-set as well as to model simulations.

Inter-decadal variability of the circulation of the North Atlantic can be characterized by the North Atlantic Oscillation (NAO) index. Hurrell's (1995) analysis suggests

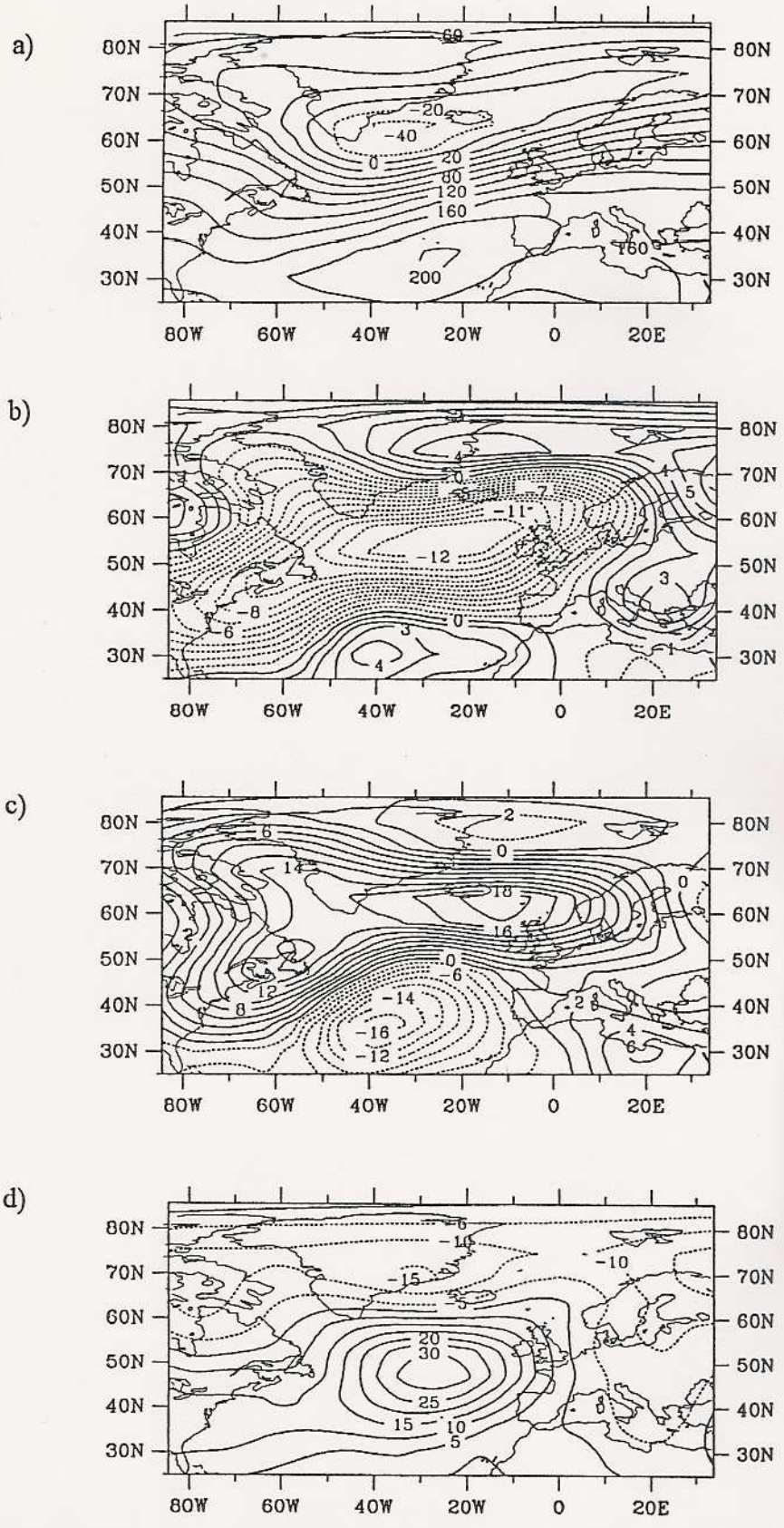

Figure 10. Geopotential height field z1000 of (a) the five-winter average and composite deviations from the mean for (b) north-eastward, (c) zonal and (d) inactive regimes of North Atlantic cyclone tracks.

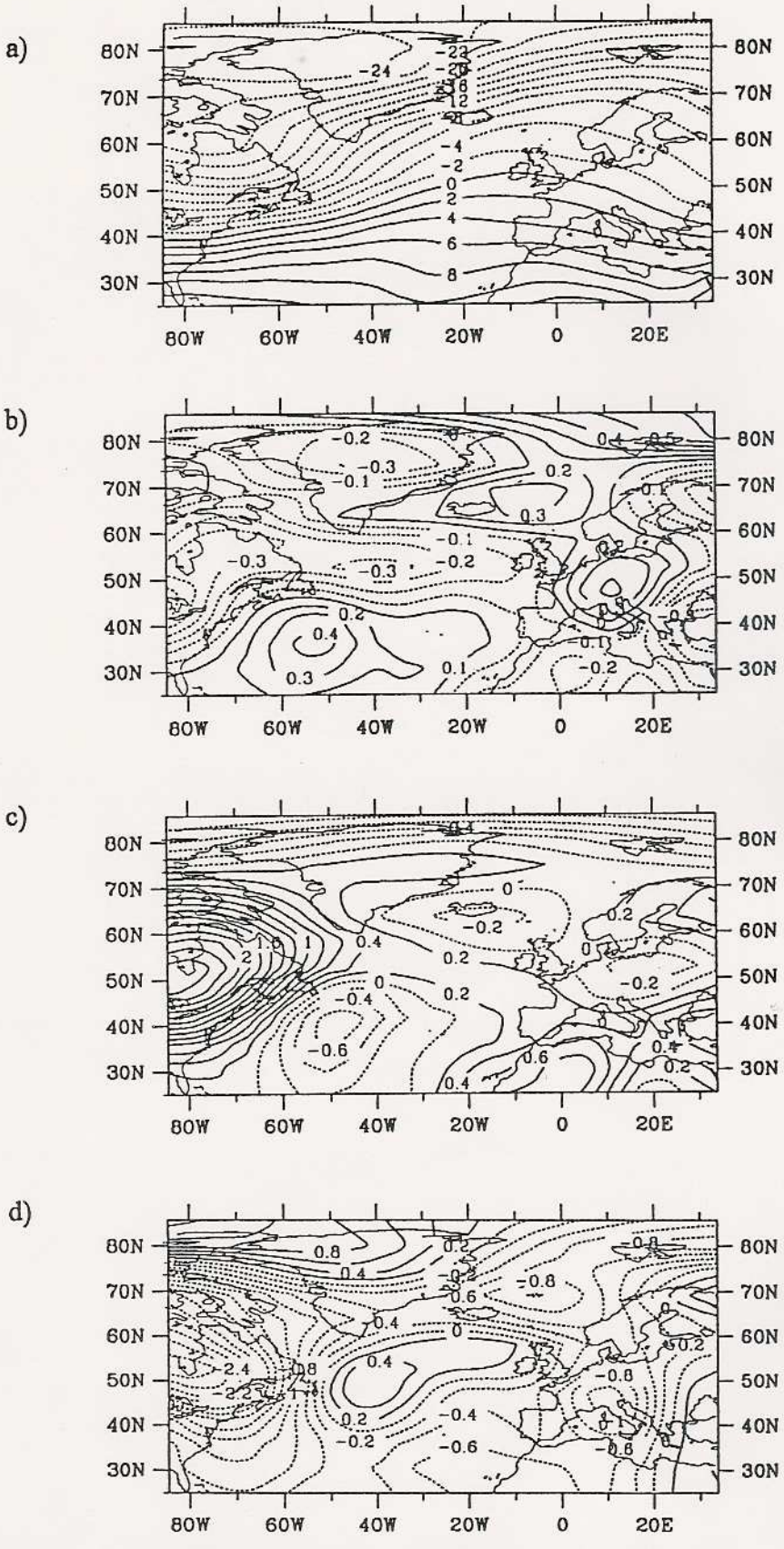

Figure 11. Temperature field (850 hPa) of (a) the five-winter average and composite deviations from the mean for (b) north-eastward, (c) zonal and (d) inactive cyclone-track regimes.

TABLE 1. NUMBER OF CASES COMPRISING THE CLUSTERS OF ZONALLY- AND NORTH-EASTWARD-TRAVELLING, AS WELL AS STATIONARY CYCLONES, IN WINTER SEASONS.

Winter	Zonal	North-east	Stationary
(89)90	16	31	36
90/91	23	30	38
91/92	12	26	48
92/93	14	25	74
93/94	13	23	72

a link between the variability of the winter-mean NAO index and the fluctuations of the moisture transport. The two dominating patterns (his Fig. 4) are associated with north-eastward (high NAO index) and with zonal moisture-fluxes (low NAO index), the mean directions corresponding to the principal cyclone traces shown in Fig. 7 and the ensembles in Figs. 3(b),(c). Similarity between short- and long-term variability raises the question whether it is accidental or caused by some physical mechanism.

The analysis also reveals a distinct increase of the number of stationary cyclones between the winters 1990/91 and 1992/93 (Table 1). This increase occurs in two steps, a modest one during 1991 and a larger one during 1992. This may be related to a climate change or, more likely, to a modification of the analysis procedure in the ECMWF model. Two major modifications have been made to the model according to ECMWF newsletters. In 9/1991 the resolution was increased to T213/31L, and in 1/1992 the horizontal diffusion was modified twice. This suggests that model validation and model inter-comparison are possible future applications of the methods presented here.

ACKNOWLEDGEMENTS

We would like to thank the two referees for their helpful comments and G. Bischof and C. Raible for calculating the residence times. This work was supported by the European Community under contract EV5V-CT94-0503, the Bundesministerium für Bildung, Wissenschaft, Forschung und Technologie (07VKV01/1) and the DAAD project ARC 313.

REFERENCES

Alpert, P., Neeman, B. U. and Shay-El, Y. 1990 Climatological analysis of Mediterranean cyclones using ECMWF data. *Tellus*, **42A**, 65–77

van Bebber, W. J. 1891 Die Zugstrassen der barometrischen Minima nach den Bahnenkarten der Deutschen Seewarte fuer den Zeitraum von 1870–1890. *Meteorol. Zeit.*, **8**, 361–366

Bell, G. D. and Bosart, L. F. 1989 A 15-year climatology of Northern Hemisphere 500-mb closed cyclone and anticyclone centres. *Mon. Weather Rev.*, **117**, 2142–2163

Fraedrich, K., Bach, R. and Naujokat, G. 1985 Single station climatology of central European fronts: Number, time and precipitation statistics. *Contr. Atmos. Phys*, **59**, 54–65

Fraedrich, K. and Leslie, L. M. 1989 Estimates of cyclone track predictability, I: Tropical cyclones in the Australian region. *Q. J. R. Meteorol. Soc.*, **115**, 79–92

Fraedrich, K., Grothjahn, R. and Leslie, L. M. 1990 Estimates of cyclone track predictability, II: Fractal analysis of midlatitude cyclones. *Q. J. R. Meteorol. Soc.*, **116**, 317–335

Hartigan, J. A. and Wong, M. A. 1979 Algorithm AS 136: A K-means clustering algorithm. *Appl. Statistics*, **28**, 100–108

Hay, R. F. M. 1949 'The rainfall in eastern Scotland in relation to synoptic situations'. Met. Office Prof. Note No. 98

Hess, P. and Brezowski, H. 1977 Katalog der Grosswetterlagen. *Ber. Dtsch. Wetterdienst Offenbach*, **113, Bd. 15**

Hodges, K. I. 1994 A general method for tracking analysis and its application to meteorological data. *Mon. Weather Rev.*, **122,** 2573–2586

Hurrell, J. W. 1995 Decadal trends in the North Atlantic Oscillation: Regional temperatures and precipitation. *Science*, **269,** 676–679

Klein, W. 1957 'Principal tracks and mean frequencies of cyclones and anticyclones in the Northern hemisphere'. Research paper No. 40, U.S. Weather Bureau, Washington

Koenig, W., Sausen, R. and Sielmann, F. 1993 Objective identification of cyclones in GCM simulations. *J. Climate*, **6,** 2217–2231

Lamb, H. H. 1972 'British Isles weather types and a register of the daily sequence of circulation patterns, 1861–1971'. Geophys. Mem., 116, HMSO, London

Lambert, S. J. 1988 A cyclone climatology of the Canadian Climate Centre general circulation model. *J. Climate*, **1,** 109–115

Murray, R. J. and Simmonds, I. 1991 A numerical scheme for tracking cyclone centres from digital data, Part I: development and operation of the scheme. *Australian Meteorol. Mag.*, **39,** 155–166

Richardson, L. F. 1926 Atmospheric diffusion on a distance-neighbour graph. *Proc. Roy. Soc. London*, **A110,** 709–737

Sanderson, B. G. and Booth, D. A. 1991 The fractal dimension of drifter trajectories and estimates of eddy-diffusivity. *Tellus*, **43A,** 334–349

Sinclair, M. R. 1994 An objective cyclone climatology for the southern hemisphere. *Mon. Weather Rev.*, **122,** 2239–2256

Tsinober, A. 1994 Anomalous diffusion in geophysical and laboratory turbulence. *Nonlinear Proc. in Geophys.*, **1,** 80–94

Ueno, K. 1993 Inter-annual variability of surface cyclone tracks, atmospheric circulation patterns, and precipitation patterns, in winter. *J. Meteorol. Soc. Japan*, **71,** 655–671

Viecelli, J. A. 1994 Persistence of Lagrangian trajectories in rotating two-dimensional turbulence. *J. Atmos. Sci.*, **51,** 337–352